Chapter 5

Stator-Rotor Interaction in Axial Turbine: Flow Physics and Design Perspective

Paolo Gaetani

Additional information is available at the end of the chapter

http://dx.doi.org/10.5772/intechopen.76009

Abstract

The stator-rotor interaction is an important issue in turbomachinery design when the highest performances are targeted. Different characters mark the interaction process in high-pressure or low-pressure turbines depending both on the blade height and on the Reynolds number. For small blade heights, being the stator secondary flows more important, a more complex interaction is found with respect to the high blades, where the stator blade wake dominates. In low-pressure turbines, the stator wake promotes the transition to turbulent boundary layer, allowing for an efficient application of ultra-high lift blades. First, a detailed discussion of the flow physics is proposed for high- and low-pressure turbines. Some off-design conditions are also commented. Then, a design perspective is given by discussing the effect of the axial gap between the stator and the rotor and by commenting the effects of three-dimensional design on the interaction.

Keywords: stator-rotor interaction, axial turbines, wake-wake interaction, vortex-blade interaction, high-pressure stages

1. Introduction

The design of high efficiency axial flow turbine stages has to face many challenging problems, and one of these is connected to the interaction between the stationary and the rotating rows of the machine. In high-pressure gas turbines, additional issues related to the combustor-turbine interaction take laces leading to further complexity in the design process.

The overall context for the design space is, in fact, an unsteady and three-dimensional flow field, where the Mach and the Reynolds numbers vary along the machine. High-pressure stages typically operate in high-subsonic or transonic regimes and are normally affected by

shock-induced separation on the rotor crown and unsteady stator rear loading [1]. Moreover, the high-loading, combined to the low aspect ratio of the first stage blading, drives the generation of wide swirling structures, whose mixing contributes significantly to the loss budget [2]. These secondary flows also affect the flow angle distribution and momentum redistribution inside the blade channel and their accurate prediction is fundamental for the designer of the gas turbine cooling system [3].

All of these flow structures affect the blade cascade where they are generated and the adjacent ones in the so-called stator-rotor interaction process. To make clear such a complex flow feature, all of them will be recalled and schematised according to what are available in the open literature.

The primary flow structures involved in the interaction process are the wake and the secondary flows. Many research studies have been proposed in the open literature discussing the wake and the secondary flow evolution and their parametric dependence on the typical turbomachinery parameters (among others, [4–9]).

The interaction process has been addressed in the last 20 years by many authors both for the high-pressure stages and for the low-pressure ones. Differences between high- and low-pressure stages arise for the dependence of the boundary layer and its transition on the Reynolds number.

When the high-pressure stages are of concern, the interaction takes place mainly in terms of shock wave, wake and secondary flows, leading to the so-called wake-blade and vortex-blade interaction. Thanks to the high Reynolds number and high inlet turbulence levels [10], the blade boundary layer state is less influenced by the incoming viscous structures (among others [11–21]). It has to be taken into account that also the inlet boundary layer properties may cause some pressure fluctuation on the cascade loading, as discussed in [22].

Low-pressure stages, on the contrary, are very sensitive to Reynolds number effects. The wakes coming from the upstream cascade periodically act as a trigger for the boundary layer transition from laminar to turbulent conditions. Such periodic transition, possibly re-laminarization, is beneficial in preventing the boundary layer separation and this allows for higher loading. In this context, ultra-high lift blade can be proficiently applied either to reduce the aero-engine weight or to power the fan (among others [25–28]).

All these issues have been addressed both experimentally and by proper CFD simulations; experiments require high promptness instrumentation like FRAPP (among others [29–32]) or LDV and PIV. Simulation, as well, requires high performance codes and schemes able to face the sliding of rotors with respect to the stationary components.

In order to gain a general perspective and to quote the importance of the interaction on the cascade aerodynamics, the reduced frequency concept has been introduced. It refers to the ratio between the time scale of the unsteadiness (typically: Ss/U, where Ss is the stator pitch and U is the rotor peripheral speed) and the one related to the transport of the mass flow across the device (i.e. b/Vax where b = axial chord and Vax = the mean axial velocity component). The reduced frequency definition then is: $f = (b\ U)/(S_s\ Vax)$. When $f << 1$, the process can

be considered as steady and its time variation related to U can be approximated as a sequence of steady state. When $f >> 1$, the process is dominated by the unsteadiness. Finally, when $f \approx 1$, the unsteady and quasisteady processes have the same order of magnitude and importance. In many cases, turbomachinery work is in the range of $f \approx 1$ while for example the combustor-1° stage interaction lies in the quasisteady conditions [33].

In the present contribution, the focus is given mainly to the gas turbines geometries and operating conditions, even though the same mechanism can be applied to steam stages. As already introduced by the title, the core of this contribution is devoted to the general discussion of the flow physics, rather than on the quantification and on the detailed description of the specific issues: this way, in author's opinion, once the general aspects are acknowledged, the detailed issues - as discussed in papers here referenced - can be properly understood.

Finally, the discussion will be on a single stage, constituted by a stator and a rotor, taken as a representative for the whole machine. In the case of multistage turbomachines, the flow field discharge by the rotor will affect, with the same mechanics described in the following, the subsequent stator. Additionally, there could be some "clocking" features between stators and rotors that may alter the single stage performance.

Experimental results have been taken by means of a steady five holes probe and fast response aerodynamic pressure probe (FRAPP) on the high-pressure axial turbine located at the laboratory of fluid-machinery (LFM) of the Politecnico di Milano. More information on the rig and measurement techniques is reported in [14, 15, 29, 31]. It is important to stress that the FRAPP is applied in a stationary frame and gives the phase resolved total and static pressure (and hence the Mach number) and the flow angle; then, by assuming a negligible effect of the temperature fluctuations, the relative Mach number and, by this, the relative total pressure are calculated.

CFD results have been obtained on the same HP turbine geometry by means of fluent code.

2. Stator-rotor interaction in axial stages

The stator-rotor interaction features different characters if occurred in high-pressure or low-pressure stages.

In low-pressure stages, thanks to the high blade height, the main interaction element is the wake in a general low-Reynolds environment.

On the contrary, high-pressure stages are typically characterised by small blade heights, due to the high mean density and by a stream with high Mach and Reynolds numbers and high mean temperatures.

As in all stages, the wake generated by the stator impinges on the rotor blades being an important source of interaction, but—due to the specific features of HP stages–other sources of interaction are present.

The small blade height has the primary impact of powering the effects of the secondary and clearance flows; in fact, they cannot be considered as negligible and modifies the potential flow pattern for a large amount of the blade span. From the stator-rotor interaction perspective, this feature makes the problem much more complex as an additional source of interaction takes place.

A common feature of the different kind of secondary flows is to be connected to loss cores, as found for wakes. However, secondary flows are also vortical structures and hence characterised by vorticity whose sense of rotation is different among the different vortices. Therefore, in the analysis of the interaction mechanism, this last feature has to be properly taken into account.

Mach number typically modulates the intensity and position of the swirling cores [7] and, if supersonic, sets the shock wave pattern discharged by the cascades.

The Reynolds number, typically high and for this the flow can be regarded as turbulent, mainly sets the interaction between the incoming structures and the rotor blades boundary layers.

As mentioned earlier, to aid the reader in the comprehension, the different kinds of interaction are discussed separately.

2.1. Stator wake-rotor blade interaction

The stator wake can be regarded either as a velocity defect or a loss filament.

According to the first approach, the velocity triangle composition shows a very different direction and magnitude for the relative velocity. **Figure 1** shows the triangles for the free stream and for the wake flow; it is evident how the relative velocity of the wake flow (W_W) heads towards the blade suction side, featuring also a negative incidence on the rotor blade.

According to the second approach, the wake has no streamwise vorticity associated to it, being the only vorticity present related to the Von Karman street, whose axis is parallel to the blade span. Once the wake interacts with the downstream rotor blade, it is bowed and then chopped by the rotor leading edge. Later on, it is transported inside the rotor channel, being smeared and showing two separate legs: one close to the suction side and one to the pressure side. Globally, the wake is pushed towards the rotor suction side by the cross-passage pressure field and, possibly, its suction side leg may interact with the blade boundary layer, this feature depends mainly on the rotor loading.

Figure 2 shows the wake in terms of entropy filament, as computed by CFD in 2D – 1 × 1 case. Downstream of the rotor blade, the wake typically appears as a distinct loss core close to the rotor wake or as a part of the rotor wake; this option is strictly dependent also on the axial position downstream of the rotor where the analysis is done. For this reason, in some papers [12, 13, 15–18] this mechanism is acknowledged as “wake-wake” interaction.

Being the rotor blade different in number with respect to the stator one, different rotor channels experience the interaction in different time even though the basic mechanism does not differ.

http://dx.doi.org/10.5772/intechopen.76009

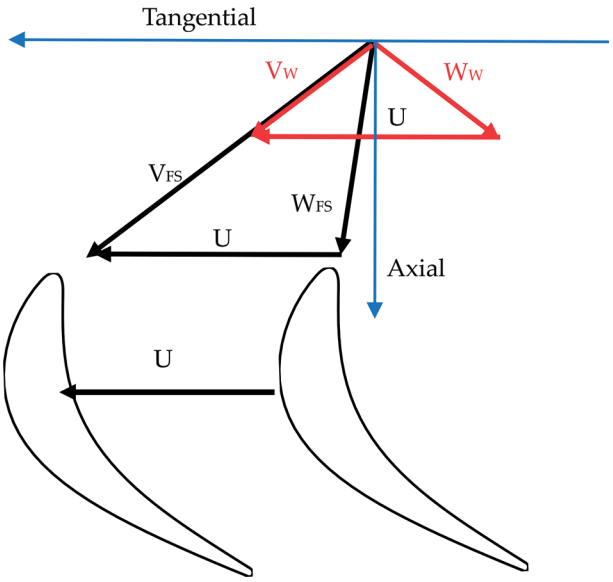

Figure 1. Velocity triangles for the free stream (subscript FS) and the wake (subscript W) flows. V = absolute velocity, W = relative velocity, U = peripheral velocity.

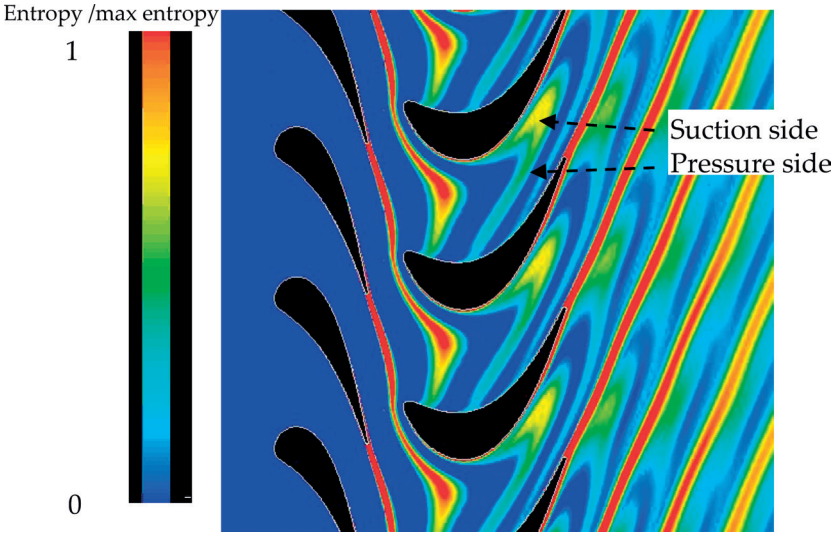

Figure 2. Pattern of entropy evolution (bowing, chopping and transport) of the stator wake in the rotor channel, as foreseen by CFD.

The rate of the interaction depends on the stator wake intensity, that is, on the stator loading, on the blade trailing edge thickness, on the axial stator-rotor gap, on the Reynolds numbers and, for cooled blade, on the kind of cooling applied.

In case of low pressure turbines, where typically the Reynolds number is low, as for the aero-engine cases, the wake – wake interaction is in fact the only effective mechanism. Its importance grows as the Reynolds number decreases and specifically, the incoming wakes, once interacting with the suction side boundary layer, promotes the laminar to turbulent transition. Such a transition, on one hand increases losses but on the other hand increases the boundary layer capability to face adverse pressure gradient and for this delaying the boundary layer separation and hence the blade stall. Thanks to this mechanism, aero-engines low-pressure stages have seen an increase of loading and for this a reduction of weight, either for a reduction of solidity or overall number of rows [25, 26].

It has to be recalled that this mechanism constitutes an aerodynamic forcing on the rotor blade whose frequency depends on the stator blade passing frequency that is in the rotating frame of reference the frequency which the rotor sees the stator wake passing ahead.

2.2. Stator secondary flows-rotor blade interaction

The basic mechanism for this kind of interaction is the same of the wake-blade one, the vortical filament is bowed, chopped and hence transported in the rotor channel. Notwithstanding such similarity, two main differences can be acknowledged. The vortical structure has its own streamwise vorticity in terms of magnitude and sense of rotation and for this a different interaction and impact with the rotor can be expected depending on the entering position in the rotor channel. Moreover, the vortex entering in the rotor channel is a flow structure specifically localised along the blade span and pitch, whereas the wake is distributed along the span.

It has to be recalled, without aiming at being exhaustive, that different swirling structures can be acknowledged downstream of the stator, as depicted in **Figure 3** and discussed in [6]. The main ones are the passage vortices, located symmetrically at tip and hub, activated by the pressure gradient across the passage and hence directed from the pressure side to the suction side. These vortices have a wide extension but typically low intensities (i.e. vorticities). At the same time, the presence of the inlet boundary layer activates also the horseshoe vortices, two legs per endwall. Coupled to each passage vortex, the shed vortex can be found, activated by the interaction between the passage vortex and the low momentum fluid belonging to the blade wake. The two passage vortices have opposite sense of rotation. The two horseshoe vortex legs have opposite sense of rotation between them and the pressure side leg is co-rotating to the corresponding passage vortex.

Passage and horseshoe vortices start their growing at the stator leading edge and continue it along the stator channel, possibly merging among them or smearing depending on the stator loading and on the inlet boundary layer thickness.

The shed vortex, being activated by the viscous transport, starts growing at the stator trailing edge at the expense of the passage vortex swirling energy, reaches its highest intensity in about half chord and then weakens due to the viscous stress that smoothens the velocity gradients. Its sense of rotation is opposite to the one of the corresponding passage vortex.

http://dx.doi.org/10.5772/intechopen.76009

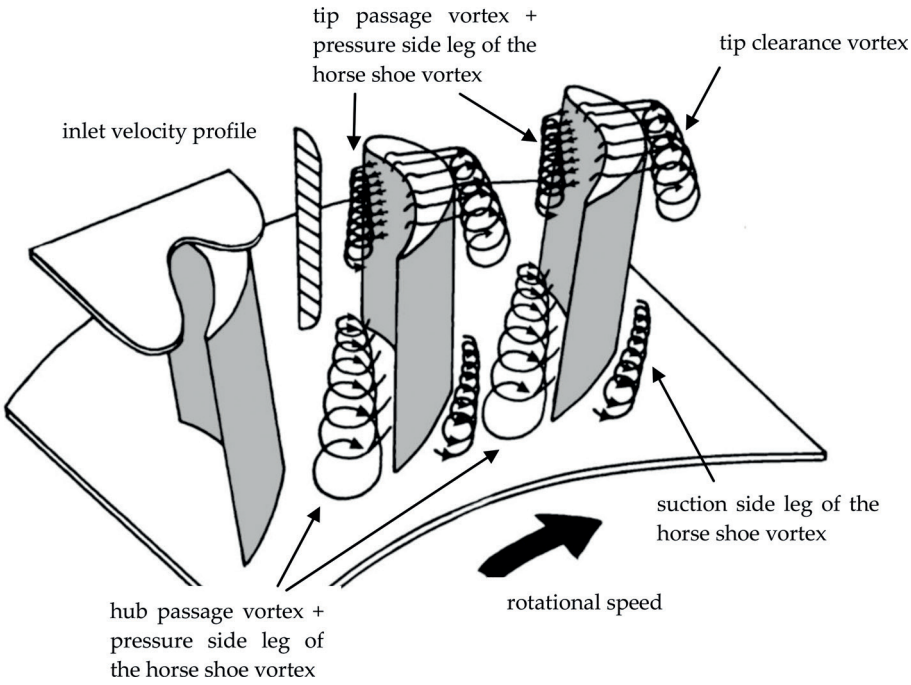

Figure 3. Simplified schematic of the secondary flows system downstream of a rotor.

Tip clearance vortex may be present depending on the sealing geometries of the stator and of the rotor. Typically, it is located at the hub in stators while it is at the tip in rotors, this latter case being much more important and frequent. Its sense of rotation is opposite to the passage vortex, being directed from the pressure side towards the suction side across the blade.

It is important to underline that all these swirling flows are present both in stators and in rotors, but with opposite sense of rotation as a consequence of the different cross pressure gradient versus in the two channels.

The secondary flow magnitude and position, besides the difference related to the tip clearance, is different between the hub and the tip. In fact, the radial equilibrium, that onsets due to the tangential component downstream of the stator, makes the static pressure at the tip higher than at the hub and for this a higher Mach number at the hub. The effect of the Mach number is well known and primarily documented by Perdichizzi [7]. Moreover, the pressure gradient acts to diffuse and to shift centripetally the vortical structures at the tip and to confine close to the endwall the hub ones.

Possible incidence angles to the stator additionally modulate the secondary flows. Positive incidence angle strengthens secondary flows, as well as lower solidities, as a consequence of the higher blade loading. Among others, a global review is reported in [8].

The flow entering the rotor is then highly three dimensional and complex, as depicted in **Figure 4**. In the case presented in **Figure 4**, by the total pressure loss coefficient and the vorticity, the passage vortices, the shed vortices and a corner vortex can be acknowledged. The Mach number map is also proposed to show the reduction due to the viscous effects of the wake and vortices and the modulation by the potential field.

To get the rotor perspective, unsteady measurements performed in the stator-rotor axial gap are reported in **Figure 5**. Such measurements, taken by FRAPP, have been plotted by applying a phase-averaging technique and a phase-lag reconstruction. The rotor pitch being smaller than the stator one, the stator wake in some instant occupies more than half of the rotor pitch, as clearly evidenced by the total pressure loss map (**Figure 5a**). The condition of constant inlet total pressure both in the absolute and in the relative frame is, so far, an unrealistic condition; **Figure 5b** shows the periodic nonuniformities throughout the relative total pressure coefficient ($C_{PT,R}$).

To aid the reader comprehension, it is first introduced that, given such complex and stator dependent flow, in this chapter, only the basic flow physics is described; in fact, the scope is to provide tools for the fluid dynamic understanding rather than a unique explanation.

As introduced at the beginning of this paragraph, the basis of the interaction between the vortex filament and the rotor blade field can be considered as not really different with respect

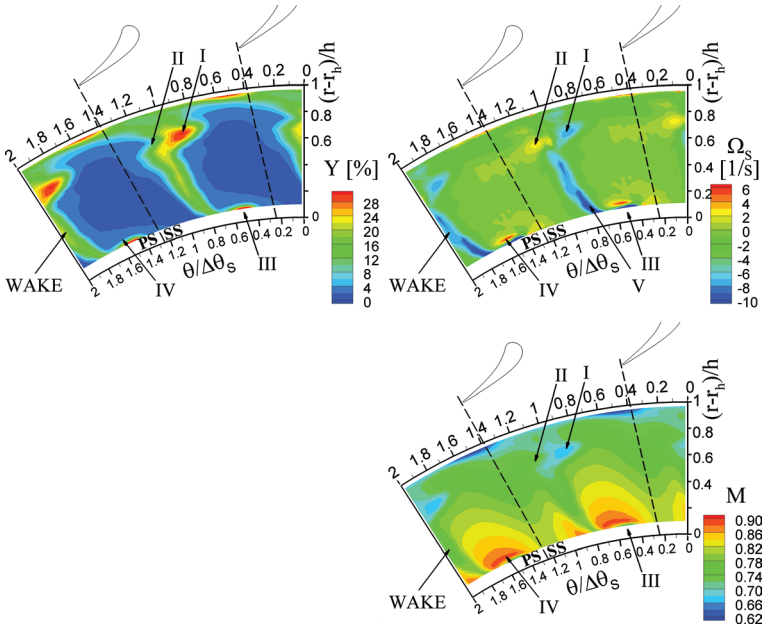

Figure 4. Total presure loss (Y%), streamwise vorticity (Ω_s) and absolute Mach number (M) downstream of the stator. Experiments at the Fluidmachinery Lab. at Politecnico di Milano (Italy).

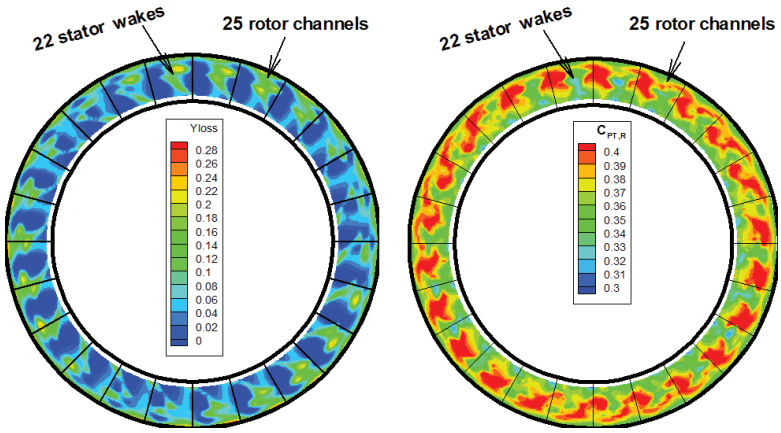

Figure 5. Rotor inlet flow field in the rotating frame of reference. Frame (a) Yloss = total pressure loss. Frame (b) $C_{PT,R}$: relative total pressure coefficient. Experiments at the Fluidmachinery Lab. at Politecnico di Milano (Italy).

to the wake one. The huge difference consists of the streamwise vorticity that characterises the vortical filament. Reader can refer to [11–13, 15–18, 20, 21] for this topic.

Once the swirling filament is bended in the rotor channel, the pressure side leg sense of rotation changes while the suction side leg preserves the original one (**Figure 6**). Moreover, being the suction side leg accelerated by the overspeed on the rotor section side, its vorticity increases; on the contrary, the pressure side leg decreases and it is smeared out along its transport.

Once the vortical structures enter the rotor channel, they interact both with the passage pressure field and with the rising vortical structure of the rotor itself. So far, the stator tip passage vortices, being opposite to the rotor one, tend to weaken it (and the same occurs for the hub ones). On the contrary, the stator shed vortex, being co-rotating with the rotor passage one will strengthen it.

Swirling flows structure entering in the rotor close to the endwalls will have stronger effects on the rotor secondary flows generations; on the contrary, the ones entering far from endwalls will interact in the downstream portion of the channel.

Moreover, the pressure side legs, as their sense of rotation is opposite with respect the original one, will undergo the opposite interaction features.

As the stator vortical structures enter the rotor periodically, with a frequency in the rotor frame equal to the stator blade passing one, the interaction process takes places periodically and this generates a pulsation of the rotor field.

Before discussing in detail the different time frames, it is straightforward to consider first the mean flow (**Figure 7a** and **b**): the $C_{PT,R}$ coefficient is in fact the total pressure in the relative frame and this evidence the loss cores generated in the rotor and in the stator. The wide low $C_{PT,R}$ region is mainly due to the rotor wake with some strengthening and enlargement due to the rotor secondary vortices (tip clearance and tip/hub passage vortex). The vortical

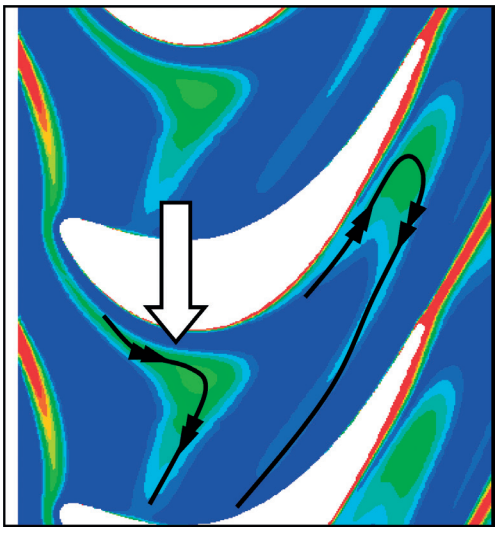

Figure 6. Skematics of the stator vortical structure transport in the rotor passage.

structures can be acknowledged by making use of the Rankine vortex model [34] applied to the deviation angle map and reported in **Figure 7b**. The clearance flow experiences a positive deviation angle as it is less deflected by the blade than the main flow. At the same time, the cross flow activated at the hub by the transversal pressure gradient, generates higher flow deflection and for this a negative deviation angle is found.

However, the time mean flow field differs from the instantaneous one due to the interaction process.

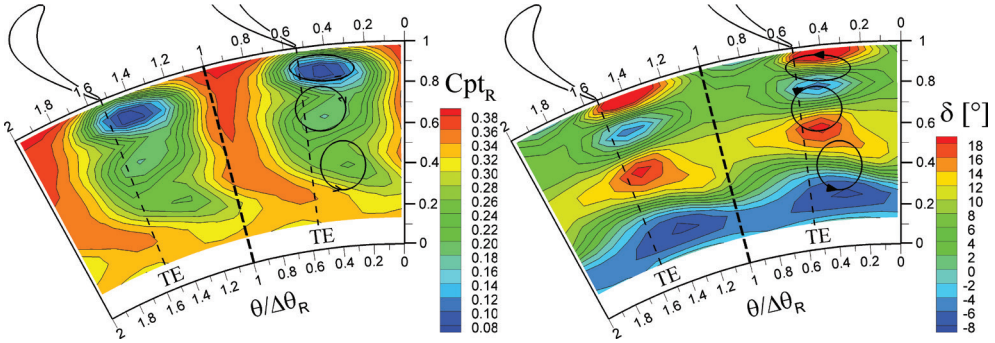

Figure 7. Time mean flow field downstream of the rotor for a subsonic operating condition (expansion ratio 1.4, reaction degree at midspan 0.3 and incidence angle close to zero). Frame (a) relative total pressure coefficient ($C_{PT,R}$); frame (b) deviation angle (δ). Experiments at the Fluidmachinery Lab. at Politecnico di Milano (Italy).

http://dx.doi.org/10.5772/intechopen.76009

Figure 8 shows different time frame of the flow field discharged by the rotor. The full rotor crown has been calculated by applying a phase leg technique to the experimental results, measured downstream of the rotor for different stator/rotor phases over one stator pitch.

It is clearly shown in **Figure 8** how the 25 channels of the turbine rotor experience different flow conditions, each of them different with respect to the time mean one.

The tip region, being dominated by the tip clearance vortex is weakly sensitive to the periodic flow evolution. On the contrary, the midspan/hub region is strongly periodically pulsating. Being the stator (n° 21) and rotor blades (n° 25) prime numbers and given that the closest periodicity is around one-thirds, the pattern evidences a periodicity every 120°.

By considering the total pressure unresolved unsteadiness, calculated as the standard deviation of the total pressure for each phase and position in the measuring plane [31], the turbulent structure can be acknowledged: for this it will be considered as the turbulence (Tu). Some of them are rotor dependent, like the rotor wake, clearance flows and rotor secondary flows; other structures, on the contrary have a clear periodic evolution with some instant where they do not exist.

Figure 9 reports different instants of the rotor evolution for three quantities: the relative total pressure coefficient, the deviation angle and the unresolved unsteadiness. With respect to the time averaged flow reported in **Figure 7** (for the same operating condition), the relative total

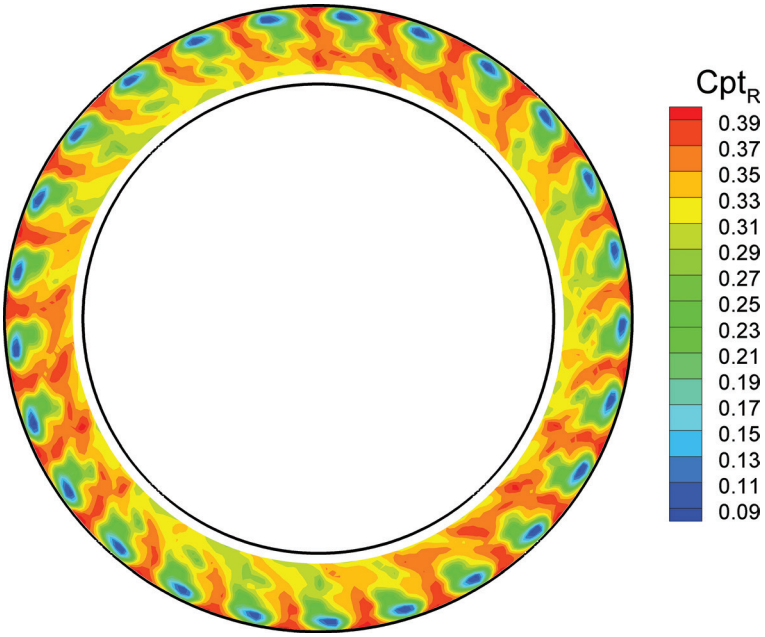

Figure 8. Relative total pressure coefficient on the whole rotor crown. Experiments at the Fluidmachinery Lab. at Politecnico di Milano (Italy).

pressure coefficient shows a fluctuating loss region, with the widest extension at t/BPP = 0.83 and the smallest one at t/BPP = 0.25, mainly in the hub region. For this latter time instant, the deviation angle shows the smallest gradient in the hub region and the unresolved unsteadiness the lowest intensity.

At t/BPP = 0.37, a vortical structure, evidenced by a high deviation angle gradient, appears in the hub region and magnifies up to t/BPP = 0.83 where its intensity is the largest. Unresolved unsteadiness and relative total pressure, mark this structure as a loss core periodically impact-

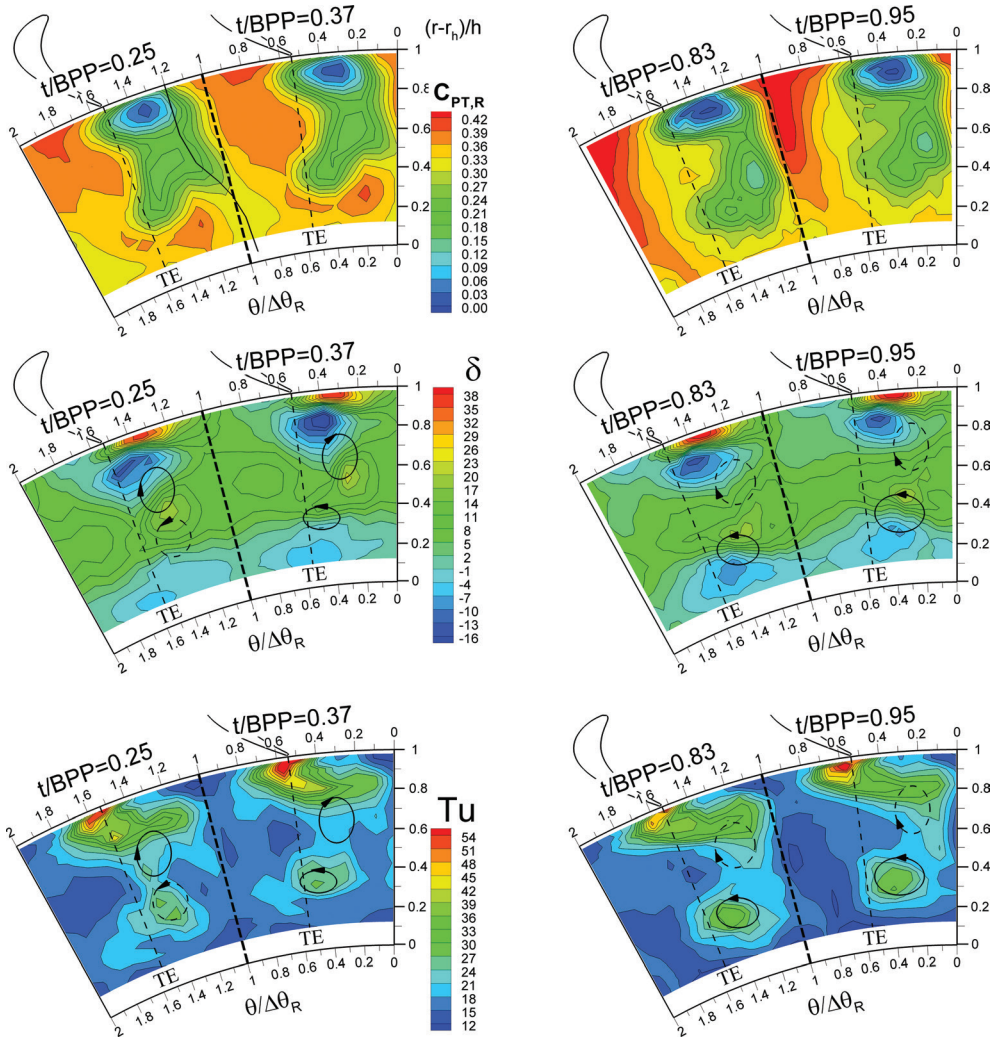

Figure 9. Relative total pressure coefficient ($C_{PT,R}$), deviation angle (δ) and turbulence (Tu) for 4 interaction phases. Experiments at the Fluidmachinery Lab. at Politecnico di Milano (Italy).

ing on the rotor channel. The sense of rotation allows accounting this phenomenon as the impact of the stator hub shed vortex, strong enough at the stator exit, on the rotor hub passage vortex.

The tip region on the contrary experiences an opposite trend with the strongest vortical structure at t/BPP = 0.25, when likely the higher inlet total pressure is found.

The highest turbulent and loss contents are found in the tip clearance region due to the high dissipation related to the clearance flow [17].

The interaction here briefly described is unfortunately for the designer case dependent where, as discussed later one, the axial gap and the loading are important issues.

To get a comprehensive perspective on the importance and on the region where the interaction takes place, the standard deviation among the different time fames is straightforward and reported in **Figure 10**. With reference to the relative total pressure coefficient, the wider fluctuations are, as qualitatively expected by **Figures 8** and **9** in the midspan-hub region. The more sensitive region at midspan is located on the wake suction side border that is the place where the stator wake interacts with the rotor one; in that region, the deviation angle evidences coherently small fluctuations. The tip region is in fact steady as the clearance flow dominates over all other structures. The hub regions, experience both variation on the total pressure coefficient and deviation angle, being the seat of the vortex/wake and vortex/vortex interaction. With reference to the deviation angle map (**Figure 10b**), the deviation angle experiences the highest fluctuation in the interface between the tip and hub passage vortex; moreover, all along the rotor wake, it fluctuates, showing the flow turning to be highly sensitive to the periodic interaction.

Off design conditions: To improve the analysis, different operating conditions are described here, being different for the incidence angle and expansion ratio. The effect of the axial gap will be discussed in the following chapter.

As the interaction depends on the rotor loading, all changes in this parameter will affect the intensity. Specifically, the increase in the rotor loading, by increasing the incidence angle, will

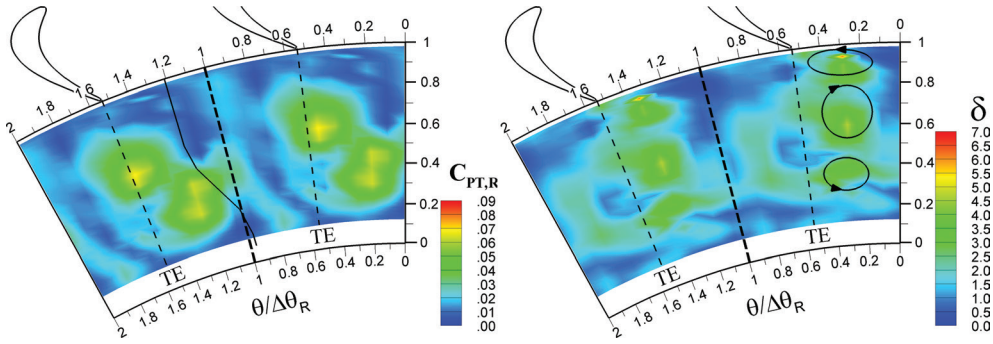

Figure 10. Standard deviation of the Cptr and δ for the different time frames. Experiments at the Fluidmachinery Lab. at Politecnico di Milano (Italy).

strengthen the interaction leaving unchanged the basic mechanism. In fact, when the rotor loading increases, the rotor suction side boundary layer is more prone to instability and the rotor vortical structure more intense, making all of them more sensitive to any variation coming from upstream. **Figure 11**, shows the relative total pressure coefficient and deviation angle standard deviations, calculated among the different time instants, for a negative incidence conditions (**Figure 11a**, incidence at midspan = −10°) and a positive one (**Figure 11b**, incidence at midspan = +10°) [35].

When the overall effect is of concern, the different interaction intensity leaves a trace on the total to total efficiency that can be summarised by stating that the higher the interaction, the lower is the efficiency.

When the fluid-dynamic forcing on the rotor blade is under study, the frequency of the forcing event is the one of the stator passing frequency multiplied by the number of swirling structures found along the pitch.

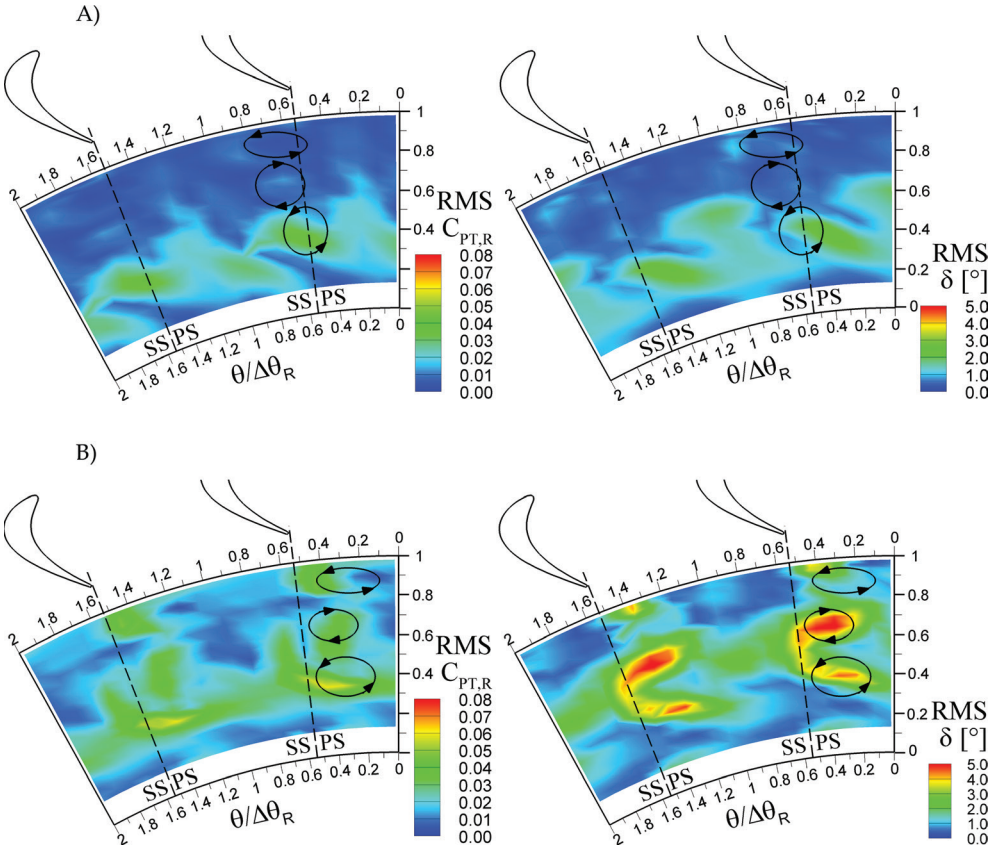

Figure 11. Rotor loading effects on the stator-rotor interaction. Experiments at the Fluidmachinery Lab. at Politecnico di Milano (Italy).

It has to be brought to the attention of the reader that the stator-rotor interaction is fundamental for the analysis of the interconnection frames, as discussed in [23] and of the turbine acoustic behaviour [24].

2.3. Stator shock-rotor blade interaction

The third possible source of interaction is related to the shocks generated at the stator trailing edge that impinge on the rotor leading edge region. Stators in high-pressure stages work often in transonic conditions at least in the hub region. Rarely, they are chocked as in this condition flow rate regulation is limited. The shock system typically has a fish-tail pattern characterised by oblique shocks; the suction side shock is stronger than the pressure side one. The suction side shock propagates downstream and interacts with the following row, while the pressure side one impinges on the adjacent blade, specifically on the suction side, being further reflected downstream.

Across the shock, the flow experiences a steep and opposite pressure gradient that, if applied to the boundary layer, acts to de-stabiles it, leading to separated flow bubbles. Thanks to the high Reynolds number, whose action is to promote the momentum exchange in the boundary layer, the effect is not that critical in high-pressure stages; it has to be recalled that rarely the outlet Mach number exceed 1.5, value where the entropy rise due to shock starts to be important.

As the stator shock sweep the rotor leading edge region, unsteadiness in the static pressure is found and for this in the boundary layer evolution; luckily, this happens where the boundary layer momentum deficit is close to be the smallest at the very beginning of the boundary layer evolution. As reported by [1, 36–38], the rotor trailing edge region is slightly affected, at least in term of static pressure and for this the boundary layer and the rotor wake are expected to be almost steady. The highest interaction is found in the leading edge/suction side region as clearly reported in **Figure 12**; the shock sweeping on the rotor leading edge first interact with the suction side of the blade (approx. in the location of measuring point n° 6, in **Figure 12**) and then reached

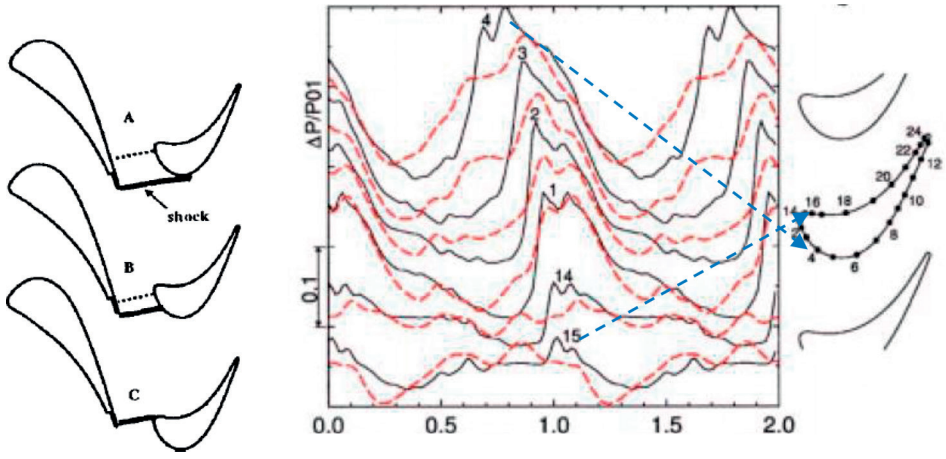

Figure 12. Vane shock-rotor interaction in axial turbine blades. Red: computation, black: experiments. Adapted from [1].

the leading edge (measuring point n° 2). The pressure side is less affected by the interaction being overshadowed by the leading edge. It is clear how the blade shape, in terms of camber/stagger angles and front/rear loading as well, it is a key parameter for this class of interaction.

The magnitude of the stator shock impinging on the rotor is strictly dependent on the axial gap; the wider it is, the weaker is the shock effect, being the shock decay rather fast.

From a mechanical perspective, the forcing induced by the stator shock on the rotor is at the stator passing frequency multiplied by the number of shocks impinging on the rotor per each stator passage, even though typically only one is important.

Other interesting studies on the interaction in transonic turbine are [39–40], where different conditions and geometries are discussed.

3. Design perspective

In general, there are a huge number of parameters that can be adjusted during the design process. Among the different parameters, some of them will be hereby described to deepen the understanding of the interaction features.

3.1. Axial gap

The axial gap is one of the key parameter for the stage optimisation. In general, the increase of the axial gap promotes the wake and secondary flows mixing and this leads to a more uniform rotor inlet flow field in the absolute frame of reference. However, the mixing increases losses and the overall total pressure level reduces. For low axial gaps, on the contrary, low-mixing takes places but a highly nonuniform flow enters in the rotor, leading to additional losses in the rotor itself. It is clear so far, how the axial gap is a parameter that has to undergo an optimisation process and this is the reason why it has been the focus of a number of research that gave different results, likely depending on the operating condition and stage loading [41].

In the context of the wide experimental campaign on the stator-rotor interaction at Politecnico di Milano, the axial gap has been also addressed and studied. The detailed discussion of the results is reported in [17], while in this context only a brief recall is proposed. Three gaps have been experimentally investigated, equal to 16, 35 and 50% of the stator axial chord. For the lowest gap case, the stator structures like wake and passage vortices are more intense than other cases and this promotes a strong interaction that results in a severe periodic fluctuation in the rotor outlet quantities. On the contrary as the gap increases, the mechanism is mainly driven by the stator shed vorticities that strengthen at the expense of the passage vortices intensities, as described in the previous paragraph. The somehow surprising result is that the lowest interaction rate is for the design case that is a gap of 35% of the stator axial chord, condition where the inlet flow field is the more uniform in terms of relative total pressure and rotor deviation angle, as clearly depicted in **Figure 13**.

For larger gaps, the combination of stator potential field and wake acts to amplify the inlet fluctuation, as reported for the incidence angle in **Figure 14**.

http://dx.doi.org/10.5772/intechopen.76009

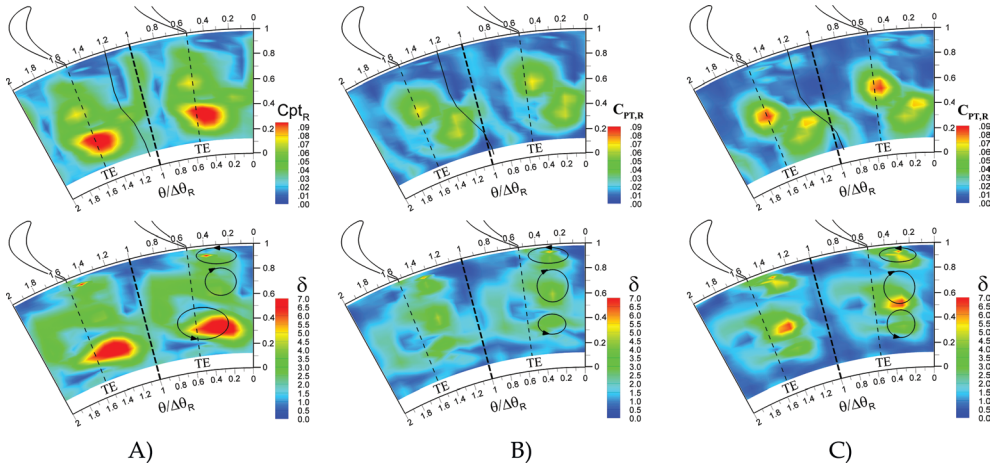

Figure 13. Standard deviation for the different instants of the interaction phases. (A) axial gap: x/bs = 16%; (B) axial gap: x/bs = 35%, nominal; C) axial gap = 50%. Experiments at the Fluidmachinery Lab. at Politecnico di Milano (Italy).

Overall, the stage experiences the maximum efficiency for the design case (**Figure 15**), about 1% higher, showing the potential of this parameter in the optimisation during the design process. According to the open literature, this trend is confirmed by some authors [42–46] but seems not general (as also reported and discussed by [41]), either for a lack of detailed data or for a case dependency in the stator wake-potential field coupling along the axial direction, in the axial gap region.

When the aerodynamic forcing is of concern, the axial gap plays a role as discussed in [47], since the forcing functions, as the wake velocity defect and the secondary flows, are stronger for low axial gaps.

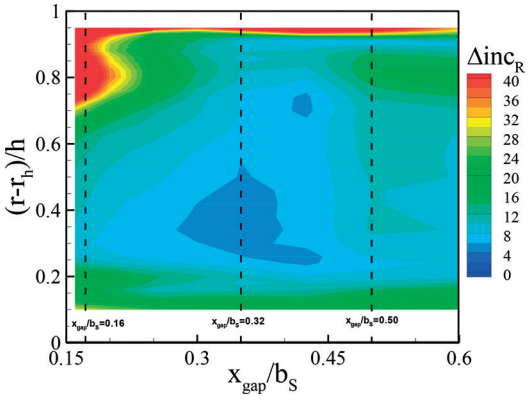

Figure 14. Rotor incidence fluctuations in circumferential direction for the differente axial gaps along the blade span.

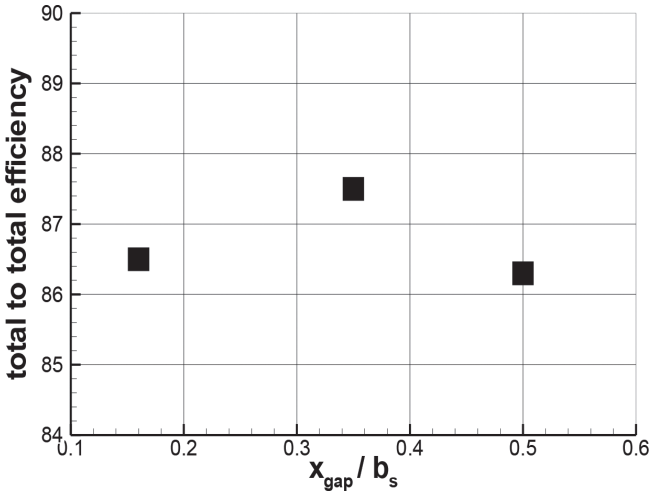

Figure 15. Efficiency trend versus the axial gap. Experiments at the Fluidmachinery Lab. at Politecnico di Milano (Italy).

3.2. Endwall contouring and 3D blade geometries

As discussed in the previous sections, the secondary flows are in the high-pressure turbine stages a leading issue for the cascade interactions. Given this matter of fact, any action devoted to the secondary flow reduction or segregation is straightforward for softening the stator-rotor interaction, aiming moreover to an overall efficiency increase.

Among the possible turbomachinery design methodologies, two of them are here briefly commented: the endwall contouring and the 3D blade design.

The **endwall contouring** consists of a specific endwall shape, at tip/hub or both, aiming at providing lower velocities in the blade portion where the highest loading is applied, that is higher turning. This feature results in a lower local cross-passage pressure gradient and a strong acceleration in the rear part of the blade. The final result is a reduction of the passage vortex in the contoured side of the passage, while the not contoured side experience about the same vortical structures [48–50].

The second possible action is the **3D blade design**. It consists of a design methodology based on a different blade stacking with respect to the conventional radial one, leading to the so-called leaned and/or bowed blades. Typically, the lean given to blades is positive that means a blade stacking inclined towards the pressure side. The bowing is given by applying a symmetrical leaning at tip and hub. These methodologies allow for a "flow control' at the cascade outlet in terms of radial pressure gradient and hence reaction. In case of positive leaning, an additional vorticity is introduced on the channel; specifically, it increases the one related to the passage vortex at the hub and smear the tip one. At the same time, the lean change the blade loading along the span by amplifying the tip one and reducing the hub one: overall such a feature makes the secondary flow at the hub less intense than the case of prismatic blades. **Figure 4** shows the vorticity field downstream of the lean annular cascade, characterised by a positive lean of 10°. When the lean is applied symmetrically at hub and tip, this benefit is gained also at tip. Overall,

the final effect in the frame of the stator/rotor interaction process is the reduction of the secondary flows and their segregation at the endwalls. This design methodology leads to an overall benefit even though the single cascade does not improve significantly its performance [51–54].

3.3. Cascades clocking

Cascades clocking refers to the design option related to the proper alignment of blades belonging to different cascades in the same frame of reference (stator/stator or rotor/rotor) in the context of multistage machines. In fact, downstream of each stage the "wake avenue' is found, that is the global effect of the stator wake and secondary flows on the rotor outlet flow field in the time mean context. This concept can be applied also to the rotor wake, when a multistage environment is considered.

To ease the understanding, let us refer to a two stages machine and specifically to the impact of the 1° stator wake avenue on the 2° stator. Depending on the kind of stages and their loading, the impact of the wake avenue can be proficiently used for increasing the following cascade efficiency. In order to clock the two different rows, cascades should have number of blades that are multiple each other and for this the design assumption of prime number have to be abandoned (it can be kept for the stator and rotor of the single stage). So far, the highest efficiency is therefore gained by using the same blade numbers between the two stators (or rotors for rotor-clocking). In LP turbines the clocking is directly linked to the wakes, while in transonic HP turbines the effect is mainly related to the interaction of wakes and secondary flows, that is the total pressure and total temperature fields on the whole, downstream the first stage with the second stator.

According to the early work from [55], the efficiency is achieved when the segments of the first vane wake avenue, released by the rotor, impinge on the leading edge of the second vane. The basic reason for this result is that the low momentum fluid coming from the first stage, collapse in the boundary layer of the second vane and for this do not affect the passage (among others, [56–58]), studied in detail the clocking effects driven by the stator secondary flows in a two stage subsonic and transonic turbines.

According to Schennach et al. [58], the interaction with secondary vortices is highly complex due to the different kind and intensity of the vortical structure itself. When the rotor structures dominate, as can happen in the tip region due to the tip clearance or for the hub secondary vortex, the clocking effect is somehow shadowed. The outer part of the channel, being typically the rotor tip passage vortex highly sensitive to the stator-rotor interaction in the upstream stage, is the place with the highest potential for the clocking. This result makes the proper alignment choice complex for the designer as it is not really general.

In case of transonic stages, the hub region, being the seat of the 1° stator shock wave and hence of the highest stator-rotor modulation, has a high potential for clocking.

As a general conclusion, when the low momentum fluid enters on the 2° stator leading edge or close to the pressure side, the highest efficiency is found. On the contrary, when the low momentum fluid coming from the 1° vane enters close to the 2° vane suction side, the lowest efficiency is found, as a consequence of the destabilising effects on the suction side boundary layer and the lowest expansion ratio there available and for this lowest suction side overspeed and for this blade lift.

Low-pressure turbines behaviour is discussed in detail in [59], where an increase of 0.7% in the efficiency is found by numerical simulations.

As a conclusive comment, the benefit achievable by clocking the cascades can be of the order of 1% in the 2° stator efficiency, being anyway highly depending on the stage features.

Nomenclature

P = pressure

$Y = (P_{T0} - P_{T1})/(P_{T1} - P_1)$: total pressure loss

$\delta = \beta_{blade} - \beta_{fluid}$: deviation angle, angles taken form the axial direction.

β = relative flow angle

$C_{PT,R} = (P_{T,R} - P_{atm})/(P_{t0} - P_{atm})$

Tu = turbulence intensity calculated by the unresolved relative total pressure [28]

V = velocity

Ω_s = streamwise vorticity: $\Omega_s = \frac{(\nabla \times \vec{V}) \cdot \vec{V}}{\|\vec{V}\|}$

Subscript

R = relative

T = total

0 = stator upstream

1 = stator downstream

Author details

Paolo Gaetani

Address all correspondence to: paolo.gaetani@polimi.it

Dipartimento di Energia, Politecnico di Milano, Milano, Italy

References

[1] Denos R, Arts T, Paniagua G, Michelassi V, Martelli F. Investigation of the unsteady rotor aerodynamics in a transonic turbine stage. ASME Journal of Turbomachinery. 2001;**123**(1):81-89

[2] Sieverding CH. Recent progress in the understanding of basic aspects of secondary flows in turbine blade passages. Journal of Engineering for Gas Turbines and Power. 1985;**107**:248-257

[3] Ong J, Miller RJ. Hot streak and vane coolant migration in a downstream rotor. Journal of Turbomachinery. 7 May 2012;**134**(5). Article number 051002

[4] Raj R, Lakshminarayana B. Characterisitcs of the wake behind a scascade of airfoils. Journal of Fluid Mechanics. 1973;**61**(4):707-730

[5] Ravindranah A, Lakshminarayana B. Mean velocity and decay characteristics of the near and far-wake of a compressor rototr blade of moderate loading. ASME Journal of Engineering for Power. 1980;**102**(3):535-548

[6] Langston LS. Secondary flows in axial turbines—A review. 2006. Annals of the New York Academy of Science. https://doi.org/10.1111/j.1749-6632.2001.tb05839.x

[7] Perdichizzi A. Mach number effects on secondary flow development of a turbine cascade. Journal of Turbomachinery. 1990;**112**:643-651. DOI: 10.1115/1.2927705

[8] Dossena V, D'Ippolito G, Pesatori E. Stagger angle and pitch-chord ratio effects on secondary flows downstream of a turbine cascade at several off-design conditions. In: Proceedings of the ASME Turbo Expo. Vienna, Austria: ASME Turbo Expo; 2004;**5**:1429-1437

[9] Boletis E, Sieverding CH, Van Hove W. Effects of a skewed inlet endwall boundary layer on the three-dimensional flow field in an annular turbine cascade. In: AGARD, CP 351; 1983. Paper No. 16

[10] Binder A. Turbulence productions due to secondary vortex cutting in a turbine rotor. ASME Journal of Engineering for Gas Turbines and Power. 1985;**107**:998-1006

[11] Dring RP, Joslyn HD, Hardin LW, Wagner JH. Turbine rotor-stator interaction. ASME Journal of Engineering for Power. 1982;**104**:729-742

[12] Chaluvadi VSP, Kalfas AI, Benieghbal MR, Hodson HP, Denton JD. Blade-row interaction in a high-pressure turbine. AIAA Journal of Propulsion and Power. 2001;**17**:892-901

[13] Pullan G, Denton JD. Numerical simulation of vortex-turbine blade interaction. In: Proceedings of the 5th European Conference on Turbomachinery; March 7-11, 2003; Prague, Czech Republic; 2003

[14] Gaetani P, Persico G, Dossena V, Osnaghi C. Investigation of the flow field in a HP turbine stage for two stator-rotor axial gaps—Part I: 3D time averaged flow field. ASME Journal of Turbomachinery. 2007;**129**:572-579

[15] Gaetani P, Persico G, Dossena V, Osnaghi C. Investigation of the flow field in a HP turbine stage for two stator-rotor axial gaps—Part II: Unsteady flow field. ASME Journal of Turbomachinery. 2007;**129**:580-590

[16] Persico G, Gaetani P, Osnaghi C. Effects of off-design operating conditions on the blade row interaction in a HP turbine stage. In: Proceedings of the ASME Turbo Expo. Montreal, Que, Canada: ASME Turbo Expo; 2007;**6**(PART A):503-517

[17] Gaetani P, Persico G, Osnaghi C. Effects of axial gap on the vane-rotor interaction in a low aspect ratio turbine stage. Journal of Propulsion and Power. 2010;**26**:325-334

[18] Persico G, Gaetani P, Osnaghi C. A parametric study of the blade row interaction in a high pressure turbine stage. Journal of Turbomachinery. 2009;**131**:031006

[19] Herbert GJ, Tiederman WG. Comparison of steady and unsteady secondary flows in a turbine stator cascade. ASME Journal of Turbomachinery. 1990;**112**:625-632

[20] Schlienger J, Kalfas AI, Abhari RS. Vortex-wake-blade interaction in a shrouded axial turbine. ASME Journal of Turbomachinery. 2005;**127**(4):699-707

[21] Pullan G. Secondary flows caused by blade row interaction in a turbine stage. Journal of Turbomachinery. 2006;**128**:484-491

[22] Hu B, Ouyang H, Jin G-Y, Du Z-H. The influence of the circumferential skew on the unsteady pressure fluctuation of surfaces of rear stator blades. Journal of Experiments in Fluid Mechanics. 2013;**27**(1):25-31

[23] Spataro R, Göttlich E, Lengani D, Faustmann C, Heitmeir F. Development of a turning mid turbine frame with embedded design—Part II: Unsteady measurements. Journal of Turbomachinery. 2014;**136**(7):071012/1-8

[24] Knobloch K, Holewa A, Guérin S, Mahmoudi Y, Hynes T, Bake F. Noise transmission characteristics of a high pressure turbine stage. In: 22nd AIAA/CEAS Aeroacoustics Conference; Lyon, France; 2016

[25] Stieger RD, Hodson HP. The unsteady development of a turbulent wake through a downstream low-pressure turbine blade passage. Journal of Turbomachinery. 2005;**127**:388-394

[26] Hodson HP, Howell RJ. The role of transition in high lift low pressure turbines. In: Effects of Aerodynamic Unsteadiness in Axial Turbomachinery, VKI Lecture Series 2005-03. 2005

[27] Lengani D, Simoni D, Pichler R, Sandberg RD, Michelassi V, Bertini F. Identification and quantification of losses in LPT cascade by POD applied to LES data, 2018. International Journal of Heat and Fluid Flow. 2018;**70**:28-40

[28] Lengani D, Simoni D, Ubaldi M, Zunino P, Bertini F, Michelassi V. Accurate estimation of profile losses and analysis of loss generation mechanism in turbine cascade. Journal of Turbomachinery. 2017;**139**:121007/1-9. DOI: 10.1115/1.4037858

[29] Persico G, Gaetani P, Guardone A. Design and analysis of new concept fast-response pressure probes. Measurement Science and Technology. 2005;**16**:1741-1750

[30] Kupferschmied P, Koppel P, Roduner C, Gyarmathy G. On the development and application of the FRAP (fast response aerodynamic probe) system for turbomachines—Part I: The measurement system. ASME Journal of Turbomachinery. 2000;**122**(3):505-516

[31] Persico G, Gaetani P, Paradiso B. Estimation of turbulence by single sensor pressure probes. In: Proceedings of the 19th Symposium of Measuring Techniques in Turbomachinery; 7-8 April 2008; Belgium: Von Karman Institute; 2008

[32] Porreca L, Hollenstein M, Kalfas AI, Abhari RS. Turbulence measurements and analysis in a multistage axial turbine. AIAA Journal of Propulsion and Power. 2007;**23**:227-234

[33] Greitzer EM, Tan CS, Graf MB. Internal Flow-Concepts and Applications. Cambridge University Press; 2004. ISBN: 0-521-34393-3

[34] Kundu PK, Cohen IM, Dowling DR. Fluid Mechanics, 5th ed. Academic Press; 2012. ISBN 978-0-12-382100-3

[35] Gaetani P, Persico G, Spinelli A. Coupled effect of expansion ratio and blade loading on the aerodynamics of a high-pressure gas turbine. Applied Sciences. 2017;**2017**(7):259. DOI: 10.3390/app7030259

[36] Paniagua G, Yasa T, de la Loma A, Castillon L, Coton T. Unsteady strong shocks interaction in a transonic turbine: Experimental and numerical analysis. Journal of Propulsion and Power. 2008;**24**(4):722-731

[37] Miller RJ, Moss RW, Ainsworth RW, Harvey NW. Wake, shock and potential field interactions in a 1.5 stage turbine—Part I: Vane-rotor and rotor-vane interaction. ASME Journal of Turbomachinery. 2003;**125**(1):33-39

[38] Tang E, Leroy G, Philit M, Demolis J. Unsteady analysis of inter-rows stator-rotor spacing effects on a transonic, low-aspect ratio turbine. In: Proceedings of the ASME Turbo Expo 2015; Montreal, Canada; 2015

[39] Rubechini F, Marconcini M, Giovannini M, Bellucci J, Arnone A. Accounting for unsteady interaction in transonic stages. Journal of Engineering for Gas Turbines and Power. 2015;**137**(5):052602/1-9

[40] Gougeon P, Boum GN. Aerodynamic interactions between a high-pressure turbine and the first low-pressure stator. Journal of Turbomachinery. 2014;**136**(7):071010

[41] Gronman A, Biester M, Turunen Saaresti T, Varri AJ, Backmann J, Seume JR. Importance of the vane exit Mach number on the axial clearance related losses. Proceedings of the Institution of Mechanical Engineers, Part A: Journal of Power and Energy. 2016;**230**(2): 175-183

[42] Dejc ME, Trojanovskij BM. Untersuchung und Berechnung Axialer Turbinenstufen. Berlin: VEB Verlag Technik; 1973

[43] Venable BL, Delaney RA, Busby JA, Davis RL, Dorney DJ, Dunn MG, Haldemann CW, Abhari RS. Influence of vane-blade spacing on transonic turbine stage aerodynamics: Part I—Time-averaged data and analysis. ASME Journal of Turbomachinery. 1999;**121**:663-672

[44] Bellucci J, Rubechini F, Arnone A, Arcangeli L, Maceli N, Paradiso B, Gatti G. Numerical and experimental investigation of axial gap variation in high-pressure steam turbine stages. Journal of Engineering for Gas Turbines and Power. 2017;**139**(5):052603/1-9

[45] Restemeier M, Jeschke P, Guendogdu Y, Gier J. Numerical and experimental analysis of the effect of variable blade row spacing in a subsonic axial turbine. Journal of Turbomachinery. 2012;**135**(2):021031

[46] Chen Y, Zhong Z, Li J, Zhou W, Zhong G, Sun Q, Ping Y, Wang S. Effect of stage axial distances on the aerodynamic performance of three-stage axial turbine using experimental measurements and numerical simulations. In: Proceedings of the ASME Turbo Expo; Charlotte, United States; 2017

[47] Jiang JP, Li JW, Cai GB, Wang J. Effects of axial gap on aerodynamic force and response of shrouded and unshrouded blade. Science China Technological Sciences. 2017;**60**(4):491-500

[48] Dossena V, Perdichizzi A, Savini M. The influence of Endwall contouring on the performance of a turbine nozzle guide vane. Journal of Turbomachinery. 1999;**121**:200-208

[49] Kopper FC, Milano R, Vanco M. Experimental investigation of endwall profiling in a turbine blade cascade. AIAA Journal. 1981;**19**(8):1033-1040

[50] Moustapha SH, Williamson RG. Effect of two Endwall contours on the performance of an annular nozzle cascade. AIAA Journal. 1986;**84**(9):1524-1530

[51] Denton JD, Xu L. The exploitation of three dimensional flow in turbomachinery design. IMechE Journal of Mechanical Engineering Science. 1999;**213**:125-137

[52] D'Ippolito G, Dossena V, Mora A. The influence of blade lean on straight and annular turbine cascade flow field. In: Proceedings of the ASME Turbo Expo. Berlin, Germany: ASME Turbo Expo; 2008;**6**(PART B):11

[53] Harrison S. The influence of the blade lean on turbine losses. Journal Turbomach. 1992;**114**(1):184-190. DOI: 10.1115/1.2927982

[54] Havakechian S, Greim R. Aerodynamic design of 50 percent reaction steam turbine. Journal of Mechanical Engineering Science. 1999;**213**:1-25

[55] Huber FW, Johnson PD, Sharma OP, Staubach JB, Gaddis SW. Performance improvement through indexing of turbine airfoils: Part 1—Experimental investigation. ASME Journal of Turbomachinery. 1996;**118**:630-635

[56] Haldeman CW, Dunn MG, Barter JW, Green BR, Bergholz RF. Experimental investigation of vane clocking in a one and one-half stage high pressure turbine. Journal of Turbomachinery. 2005;**127**(3):512-521

[57] Behr T, Kalfas AI, Abhari RS. Stator-clocking effects on the unsteady interaction of secondary flows in 1.5 stage unshrouded turbine. Proceedings of the Institution of Mechanical Engineers, Part A: Journal of Power and Energy. 2007;**221**:779-792

[58] Schennach O, Woisetschläger J, Paradiso B, Persico G, Gaetani P. Three dimensional clocking effects in a one and a half stage transonic turbine. Journal of Turbomachinery. 2010;**132**(1):011019. 1-10. Inglese

[59] Arnone A, Marconcini M, Pacciani R, Schipani C, Spano E. Numerical investigation of airfoil clocking in a three-stage low-pressure turbine. Journal of Turbomachinery. 2002;**124**:61-68